

Supernova Blastwaves in Low-density Hot Media: a Mechanism for Spatially Distributed Heating

Shikui Tang and Q. Daniel Wang

*Department of Astronomy, University of Massachusetts, Amherst, MA 01003
tangsk@astro.umass.edu and wqd@astro.umass.edu*

ABSTRACT

Most supernovae are expected to explode in low-density hot media, particularly in galactic bulges and elliptical galaxies. The remnants of such supernovae, though difficult to detect individually, can be profoundly important in heating the media on large scales. We characterize the evolution of this kind of supernova remnants, based on analytical approximations and hydrodynamic simulations. We generalize the standard Sedov solution to account for both temperature and density effects of the ambient media. Although cooling can be neglected, the expansion of such a remnant deviates quickly from the standard Sedov solution and asymptotically approaches the ambient sound speed as the swept-up thermal energy becomes important. The relatively steady and fast expansion of the remnants over large volumes provides an ideal mechanism for spatially distributed heating, which may help to alleviate the over-cooling problem of hot gas in groups and clusters of galaxies as well as in galaxies themselves. The simulations were performed with the FLASH code.

Subject headings: cooling flows — galaxies: ISM — galaxies: clusters: general — ISM: structure — supernova remnants

1. Introduction

Supernovae (SNe) are a major source of the mechanical energy input in galaxies and possibly in the intergalactic medium (IGM). On average, an SN releases about 10^{51} ergs of kinetic energy carried by the ejecta which drive a blastwave into the ambient medium. How far this blastwave goes and how fast the energy is dissipated depend sensitively on the density and temperature of the medium. Core-collapsed SNe represent the end of massive stars, the bulk (if not all) of which form in OB associations. The energy release from such an association, highly correlated in space and time, has a great impact on the surrounding

medium. Initially, the energy release from the OB association is primarily in form of intense ionizing radiation from very massive stars, which tends to homogenize the surrounding medium (McKee et al. 1984). After a couple of 10^6 years, fast stellar winds start to play a major role in heating and shaping the medium, creating a low-density hot bubble (Weaver et al. 1977), probably even before the explosion of the first SN in the association. Later, after about 5×10^6 years of the star formation (if more-or-less coeval), core-collapsed SNe become the dominant source of the mechanical energy input into the already hot surrounding (Monaco 2004). This combination of the concerted feedbacks, lasting for $\sim 5 \times 10^7$ years — the lifetime of an $8M_{\odot}$ star, leads to the formation of a so-called superbubble of low-density hot gas enclosed by a supershell of swept-up cool gas (e.g., Mac Low & McCray 1988). The expansion of such a superbubble is expected to be substantially faster than typical OB association internal velocities of a few km s^{-1} . Therefore, a majority of core-collapsed SNe ($\sim 90\%$) should occur inside their parent superbubbles (e.g., Higdon et al. 1998; Parizot et al. 2004 and references therein). SNe from lower mass stars (e.g., Type Ia; e.g., McMillan & Ciardullo 1996), particularly important in early-type galaxies and possibly in galactic bulges and halos, are also expected to occur mostly in low-density hot media. The interstellar remnants of such SNe are typically too faint to be well observed individually. But in terms of both heating and shaping the global ISM/IGM, such “missing” remnants are probably more important than those commonly-known and well-studied supernova remnants (SNRs). Though spectacular looking, they are atypical products of SNe (e.g., from run-away massive stars), which happened to be in relatively dense media.

Surprisingly, there has been little work toward the understanding of the SNR evolution in hot media with relatively high pressure. Almost all the existing studies assume an ambient medium with both low temperature and low pressure (e.g., $T \lesssim 10^4 \text{ K}$, $nT \lesssim 10^4 \text{ cm}^{-3}\text{K}$; Chevalier 1974; Cioffi et al. 1988; Shelton 1999) or relative high in temperature but still low in pressure (e.g, $T \sim 10^{6-7} \text{ K}$, $nT \sim 10^{3-4} \text{ cm}^{-3}\text{K}$; Dorfi & Volk 1996). If both the ambient gas temperature and pressure are low (e.g., $T \lesssim 10^4 \text{ K}$, $nT \lesssim 10^4 \text{ cm}^{-3}\text{K}$), much of the SNR evolution may then be described by the self-similar Sedov solution (Sedov 1959), which assumes that both the thermal energy and radiative cooling of swept-up gas are negligible. The ambient gas with both high temperature and high pressure makes two differences: (1) the shock is weak due to the high sound speed and (2) thermal energy of the swept-up gas is not negligible. Sedov (1959, P238-251) made a linear approximation to the pressure effect, but did not account for the high temperature effect (Gaffet 1978). Dorfi & Volk (1996) briefly mentioned the behavior of an SNR shock asymptotically reaching the sound speed, but studied primarily the cosmic ray acceleration. McKee & Ostriker (1977) considered the SNR evolution in a cloudy medium, including thermal evaporation. Although the intercloud medium in this case is hot ($T \sim 10^6 \text{ K}$), the average ambient pressure is still low

($nT \sim 10^3 \text{ cm}^{-3}\text{K}$). The characteristic temperature and pressure inside galactic bulges and elliptical galaxies are about 2~3 orders of magnitude higher than the values used in these SNR studies (Spergel & Blitz 1992; Morris & Serabyn 1996 and references therein). Shigeyama & Fujita (1997) simulated an SNR in a hot medium with relative high pressure ($n = 0.1\text{cm}^{-3}$ and $T \approx 10^7 \text{ K}$), but focused only on the ejecta. In short, we are not aware of any simple description or simulation of the SNR evolution in the hot media typically for galactic bulge and elliptical galaxies.

We have closely examined the SNR evolution in the relatively low-density and high pressure hot media. The evolution of such an SNR is significantly different from those in a relatively dense and cold environment. While the low density means that the SN energy loss rate is slow, the high pressure makes the swept-up thermal energy dynamically important. Furthermore, the expansion speed of the blastwave is always above the sound speed of the hot ambient medium with the value of a few hundred km s^{-1} . Therefore, the SNR can expand to a large volume and distribute its energy in a rather uniform fashion. In the following, we demonstrate these effects, based chiefly on 1-D high-resolution hydrodynamic simulations.

2. Simulation Setup

Our simulations use the newly released FLASH code (version 2.4), which allows for modular, adaptive-mesh, and parallel simulations and solves the hydrodynamic equation explicitly (Fryxell et al. 2000 and references therein) To accurately capture a shock front, we use a uniformly spaced grid with a spatial resolution of about 0.01 pc. We assume that the SN explosion is spherically symmetric and the ambient medium is uniformly distributed with identical temperature (T_0) and density ($\rho_0 = n_0 m_p$). The number density of particles is $n = n_0/\mu$ where $\mu \approx 0.6$ for fully ionized gas with the solar abundance. An SN energy E_{sn} ($= 10^{51}$ ergs) is deposited inside a small radius r_{init} . The ambient gas is assumed to be mostly ionized. The cooling is neglected in the simulations (further discussion in §4). Table 1 lists the setup parameters (T_0 , n_0 and r_{init}) of a few representative cases, which are characteristic of the Galactic bulge (A), giant elliptical galaxies (B), and rich clusters of galaxies (C). The table also lists various inferred parameters to be discussed in the following sections.

We have experimented with various energy deposition schemes (Cioffi et al. 1988; Chevalier 1974). If the explosion energy is initially deposited as heat uniformly in a small volume, a Sedov solution can be quickly reached. On the other hand, depositing the energy in the form of kinetic energy leads to many small-scale structures due to various internal shocks especially inside the ejecta. With or without ejecta (assumed to have a total mass of 1.4

M_\odot) do affect the evolution before the swept-up mass becomes dominant compared with the ejecta. However, a specific choice of the initial conditions does not significantly affect our conclusion on the overall structure and evolution of the SNRs.

We output simulation results every 100 years. The radius of the outer shock front (R_s) corresponds to the position where the gradients of the pressure and velocity are the largest. The shock front velocity (V_s) is estimated from the R_s difference between two consecutive steps. Therefore, the accuracy of the local R_s and V_s estimates is limited by the finite resolution in both time and spatial step sizes. An adaptive smooth of the V_s evolution is performed to reduce the step-by-step fluctuation. The uncertainties in these calculations in individual steps do not affect the actual *evolution* of these parameters, which are determined by the internal hydrodynamic solutions in the simulations.

3. Results: Outer Blastwave Evolution

Figure 1 shows the evolution of R_s and V_s for the three cases listed in Table 1. In all cases, the initial free-expansion stage is short and ends when the swept-up mass roughly equals to that of the ejecta. The expansion then more-or-less follows the self-similar Sedov solution:

$$V_{Sedov} = \frac{2}{5}\xi \left(\frac{E_{sn}}{\rho_0 t^3} \right)^{1/5}, \quad (1)$$

where $\xi=1.14$ for gas with $\gamma=5/3$. But, the Sedov phase does not last long if the ambient medium has a high temperature. The evolution gradually deviates from the Sedov solution, as the blastwave expansion asymptotically approaches the sound speed of the ambient medium. Based on these asymptotical behaviors (neglecting the brief free-expansion phase), we find that the following expression gives a simple generalization of the Sedov solution, approximately characterizing the blastwave evolution in a low-density hot medium (to an accuracy of $\lesssim 3\%$; see the bottom panels of Figure 1):

$$V_s = c_s \left(\frac{t_c}{t} + 1 \right)^{3/5} \quad (2)$$

where c_s is the sound speed of the ambient medium, and t_c is a characteristic time which can be obtained from the Sedov solution by equaling V_{Sedov} and V_s when $t \ll t_c$:

$$t_c = \left[\left(\frac{2}{5}\xi \right)^5 \frac{E_{sn}}{\rho_0 c_s^5} \right]^{1/3}. \quad (3)$$

From Eq. (2), one can easily estimate the Mach number $M = V_s/c_s$ of the blastwave as function of time, e.g., $M \approx 1.5$ at $t = t_c$ and a strong shock (i.e., $M > 2$) for $t <$

$0.46t_c$, or about a few 10^4 years. For ease of reference, Table 1 also lists the time and the swept-up ambient mass when $M = 2$. Note that Eq. (1) is not valid even before $t = t_c$. Subsequently, the blastwave expands with a low Mach number and will eventually be dissipated by radiative cooling and turbulent motion, which cannot be accounted for here in 1-D simulations, however. But the expansion speed would not fall below the sound speed.

By integrating Eq. 2, we further derive the blastwave radius,

$$\begin{aligned} R_s(t) &= \int_0^t c_s \left(\frac{t_c}{t'} + 1 \right)^{3/5} dt' \\ &= \frac{5}{2} c_s t_c \left(\frac{t}{t_c} \right)^{2/5} F \left(-\frac{3}{5}, \frac{2}{5}; \frac{7}{5}; -\frac{t}{t_c} \right), \end{aligned} \quad (4)$$

where F is the generalized hyper-geometric function.

The characteristic parameter t_c has a clear physical meaning. Within the radius $R_c \equiv R_s(t_c) \approx 2.89c_s t_c$, the ambient thermal energy swept up by the blastwave is

$$\frac{4}{3} \pi R_c^3 \frac{n_0 k T_0}{\mu(\gamma - 1)} = \frac{0.247 \pi \xi^5}{\gamma(\gamma - 1)} E_{sn} \simeq 1.8 E_{sn}, \quad (5)$$

where $\mu=0.6$. Therefore, t_c characterizes the time when the swept-up thermal energy is about twice the explosion energy. Note that for a given E_{sn} , R_c depends only on the ambient pressure, but t_c depends on both the density and the temperature.

Eqs. (2) and (4) generalize the Sedov solution, by accounting for both temperature and density effects of the ambient medium. The temperature effect is reflected in the explicit dependence of the SNR evolution on c_s . When $c_s \rightarrow 0$ (thus $t_c \rightarrow \infty$), Eqs. (2) and (4) become the Sedov solution. In general, R_s is determined by M , which depends only on t/t_c (Eq. 2), and R_c . In other words, M is uniquely determined by R_s for a given R_c . Eqs. (2) and (4) show that both V_s and R_s could have substantially larger values than what are predicted by the Sedov solution, while M is generally low. Therefore, the SNR blastwave heating is locally gentle and is over a large volume in the low-density hot medium.

4. Results: Interior Structure of the Supernova Remnants

Figure 2 illustrates the radial structure of our simulated SNRs (Case A as an example). At the early stage (before time a) the SNR maintains a strong shock and the post-shock gas moves forward at a speed greater than the sound speed of the ambient gas. A low pressure region gradually develops inside the SNR due to the adiabatic expansion, as shown in the

pressure panel. Remarkably, both density and temperatures can fall below the ambient values. Therefore, the cooling rate, hence the X-ray emission, of this region can be very low. The pressure at the SNR center reaches the minimum at time b. Later, the post-shock gas starts to flow back and the central pressure increases, gradually approaching the value of the ambient medium (time c-e). But, the under-pressure region behind the widening blastwave front remains. Figure 3 shows the conversion of the explosion energy to the thermal and kinetic energy of the swept-up medium as a function of time, which depends weakly on the specific initial conditions except for the first several 10^3 years (§2). In addition to the explosion energy, the blastwave also redistributes the thermal energy of the swept-up ambient medium.

While the energies are redistributed widely, the ejecta are confined within relatively small regions. Figure 1 (left-hand panel) includes the evolution of the contact discontinuity between the ejecta and the swept-up ambient medium of Case A with $1.4 M_{\odot}$ ejecta. The discontinuity reaches a maximum of only ~ 10 pc, consistent with the result of Shigeyama & Fujita (1997). Therefore, the metal enrichment of an SNR may still be localized even in a low density medium, unless an interaction with another SNR or a global flow such as a galactic wind redistributes the ejecta.

We have neglected the cooling effect. Using the collisional ionization equilibrium (CIE) cooling rate, we estimate the total radiative energy loss to be less than 5% up to 0.2 Myr. The undisturbed ambient gas itself radiates even more efficiently than the swept-up gas by SN blastwave. The potential deviation from the assumed CIE should be small, because the ambient medium considered here is already highly ionized.

5. Discussions

The above results show that the evolution of an SNR in a low-density hot medium has several distinct properties: 1) The blastwave always moves at a speed greater than, or comparable to, the sound wave and can thus reach a much larger radius than that predicted by the Sedov solution; 2) Because the remnant never gets into a snow-plow radiative phase, the radiative cooling is typically negligible; 3) The swept-up thermal energy is important, affecting the evolution of both the blastwave and the interior structure; 4) Because the Mach number of the blastwave is typically small, its heating is subtle and over a large volume.

The large-scale distributed heating by such SNRs may have strong implications for solving the energy balance problems in studying diffuse hot gas. The most notable problem is perhaps the apparent lack of predicted cooling flows in groups and clusters of galaxies

(Mathews & Brighenti 2003; Peterson et al. 2003). Various existing proposals for the solution (e.g., AGN heating and thermal conduction) have only limited success and many uncertainties. Fundamentally, a distributed heating mechanism is required to balance the cooling (e.g. Roychowdhury et al. 2004). Indeed, heating due to sound waves generated by buoyant bubbles from AGN energy injections has recently been proposed as a solution (Ruszkowski et al. 2004a,b). But none of these proposals are likely to explain the more acute over-cooling problem in individual galaxies, where the cooling time scale of hot gas is even shorter. As shown above, blastwaves produced by SNe, Type Ia in particular, may provide a natural mechanism for the heating required to balance, or at least alleviate, the cooling of the diffuse hot gas around individual galaxies, possibly even in the IGM (Domainko et al. 2004).

Clearly, the above discussion is very much limited by our 1-D simulations of individual SNRs. We are currently carrying out 3-D simulations to study the evolution of hot gas in galactic bulges. These simulations will account for the cooling as well as the spatial inhomogeneity generated by the global galactic gravity and by the interaction among multiple SNRs. The spatial distribution and physical properties of the gas will then be determined self-consistently.

Acknowledgments. We thank R. A. Chevalier, J. Slavin, R. Shelton, and the anonymous referee for useful comments on the work, which is supported by NASA through grant G03-4111X. The software used in this work was in part developed by the DOE-supported ASC / Alliance Center for Astrophysical Thermonuclear Flashes at the University of Chicago.

REFERENCES

- Chevalier, R. A. 1974, ApJ, 188, 501
- Cioffi, D. F., Mckee, C. F., & Bertschinger, E. 1988, ApJ, 334, 252
- Domainko, W., Gitti, M., Schindler, S., & Kapferer, W. 2004, A&A, 425, L21
- Dorfi, E. A., & Volk, H. J. 1996, A&A, 307, 715
- Fryxell, B., et al. 2000, ApJS, 131, 273
- Gaffet, B. 1978, ApJ, 225, 442
- Higdon, J. C.; Lingenfelter, R. E.; Ramaty, R. 1998, ApJL, 509, 33
- Mac Low, M.-M., & McCray, R. 1988, ApJ, 324, 776

- McMillan, R. J., & Ciardullo, R. 1996, *ApJ*, 473, 707
- Mathews, W. G., & Brighenti, F. 2003, *ARA&A*, 41, 191
- McKee, C. F., & Ostriker, J. P. 1977, *ApJ*, 218, 148
- McKee, C., Van Buren, D., & Lazareff, B. 1984, *ApJL*, 278, 115
- Monaco, P. 2004, *MNRAS*, 354, 151
- Morris, M., & Serabyn, E. 1996, *ARA&A*, 34, 645
- Ostriker, J. P., & McKee C. F. 1988, *Rev. Mod. Phys.*, 60, 1
- Parizot, E., et al. 2004, 2004, *A&A*, 424, 747
- Peterson, J. R., et al. 2003, *ApJ*, 590, 207
- Roychowdhury, S., et al. 2004, *ApJ*, 615, 681
- Ruszkowski, M., Brüggén, M., & Begelman, M. C. 2004a, *ApJ*, 611, 158
- Ruszkowski, M., Brüggén, M., & Begelman, M. C. 2004b, *ApJ*, 615, 675
- Sedov, L. I. 1959, *Similarity and Dimensional Methods in Mechanics* (New York: Academic Press)
- Shelton, R. L. 1999, *ApJ*, 521, 217
- Shigeyama, T., & Fujita, Y. 1997, in *X-Ray Imaging and Spectroscopy of Cosmic Hot Plasmas*, Waseda University, Tokyo, Eds: F. Makino & K. Mitsuda, p191
- Spergel, D. N., & Blitz, L. 1992, *Nature*, 357, 665
- Weaver, R., McCray, R., Castor, J., Shapiro, P., & Moore, R. 1977, *ApJ*, 218, 377

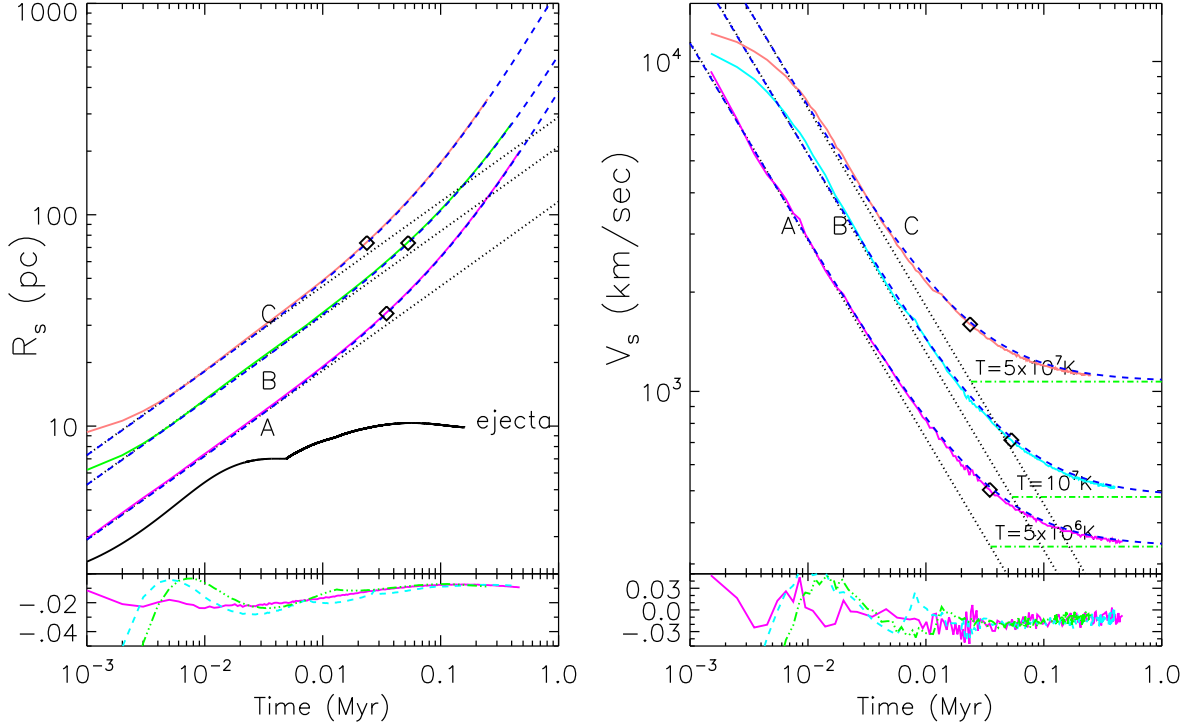


Fig. 1.— The evolution of R_s (left-hand panel) and V_s (right-hand panel) for three cases. The colored (light) solid curves, marked with Case A, B, and C (Table 1), are the simulation results; dotted straight lines are the corresponding analytic Sedov solutions. The heavy solid curve in the right panel represents the evolution of the contact discontinuity. The diamond marks the values of R_s and V_s at time t_c . The horizontal dash-dotted lines in the right-hand panel denote the corresponding sound velocities of ambient media. The bottom of each panel shows the relative error of the simulated results to the generalized analytic approximations (Eqs. 2 and 4) for Case A (solid curve), B (dashed curve), and C (dash-dot-dotted curve).

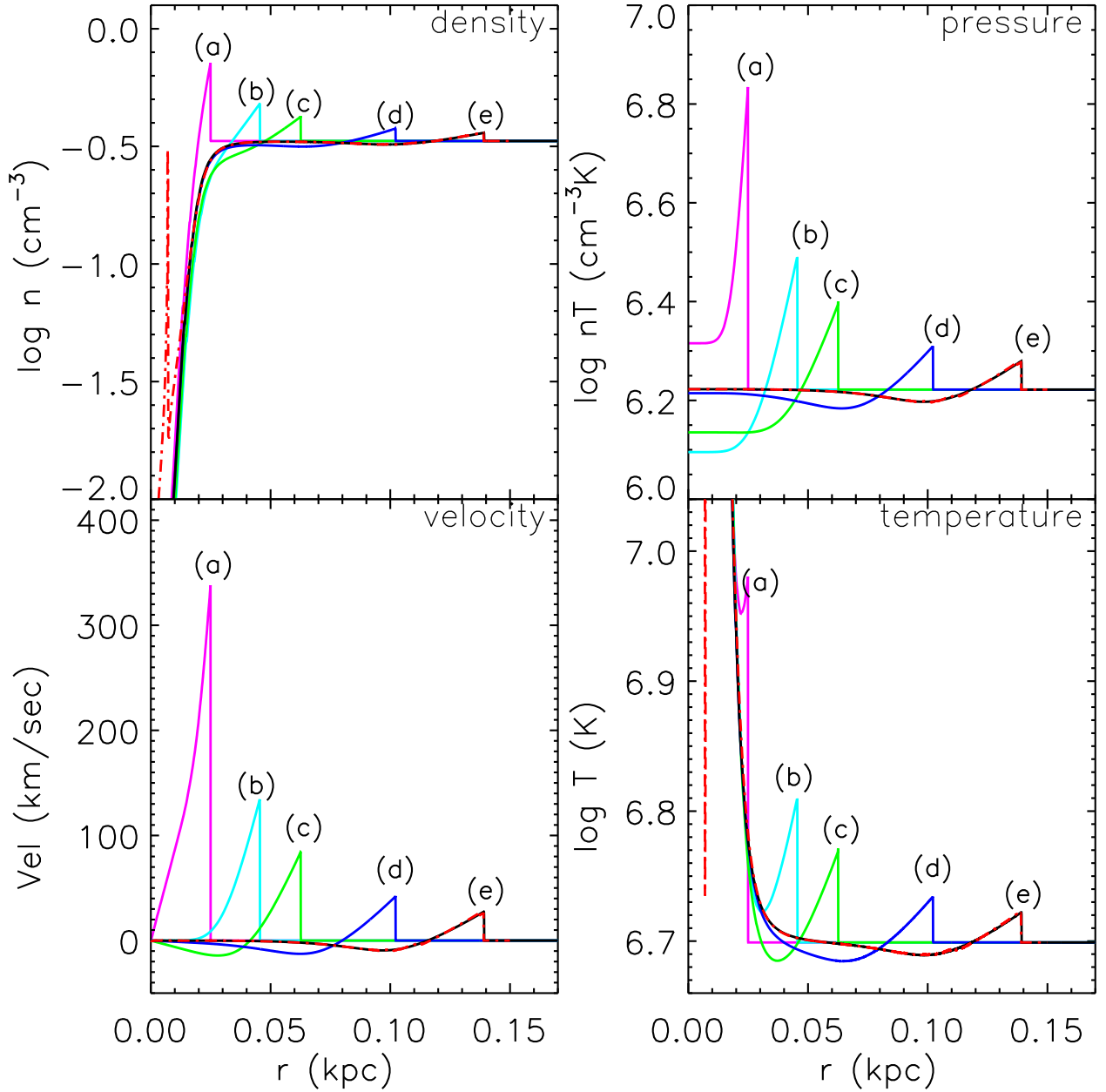


Fig. 2.— Solid curves show the structures of Case A with energy deposited as pure thermal energy at (a) 0.018/1.87, (b) 0.058/1.33, (c) 0.098/1.20, (d) 0.20/1.10, and (e) 0.30/1.07 Myr/Mach number. For comparison, the dash-dotted (red) line illustrates the result at the same time as (e) from a simulation in which E_{sn} is deposited in form of kinetic energy.

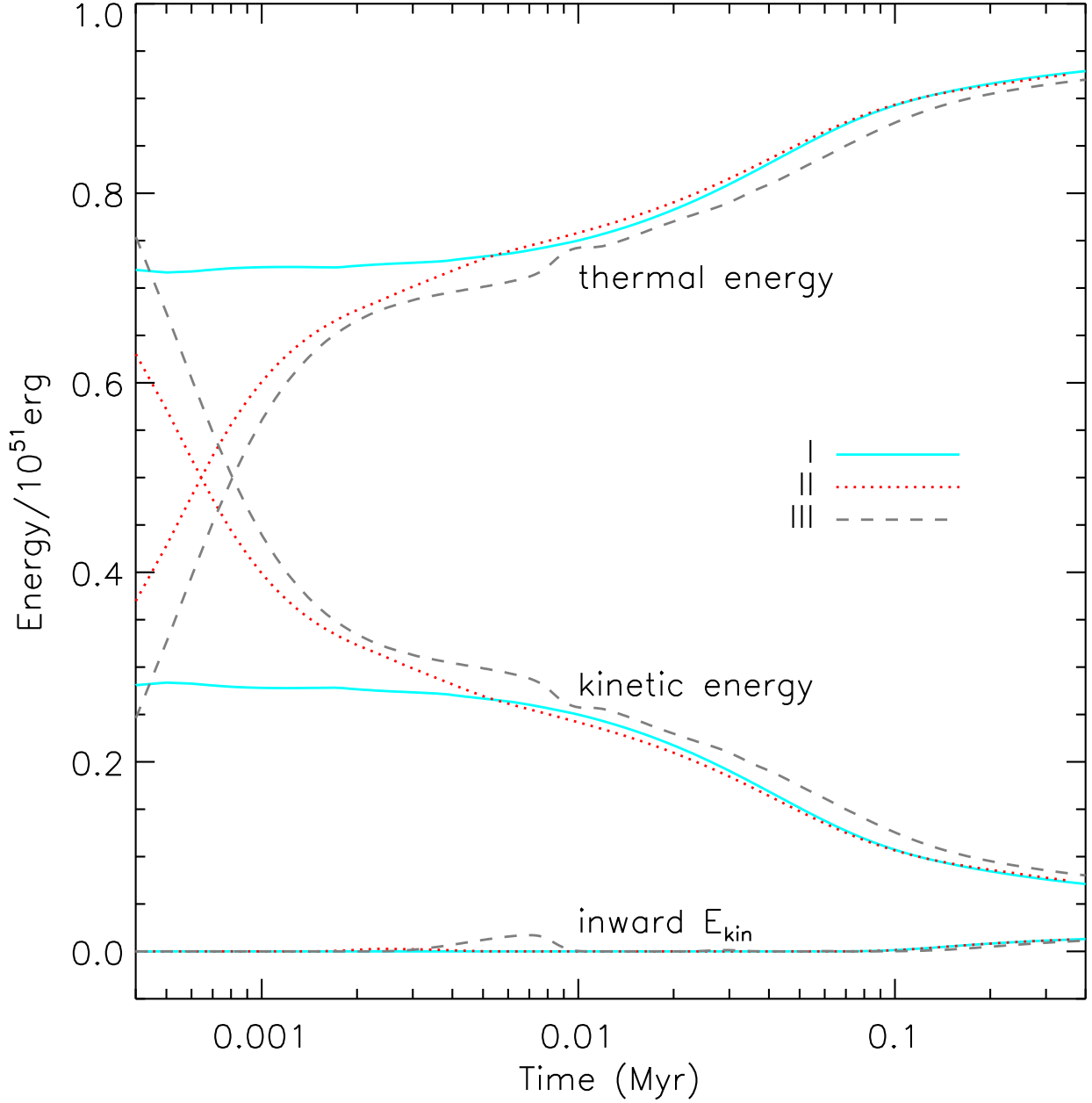


Fig. 3.— The evolution of thermal and kinetic energies of Case A SNR: I — E_{sn} as pure thermal energy without ejecta; II — E_{sn} as pure thermal energy with $1.4 M_{\odot}$ ejecta; and III — E_{sn} as kinetic energy with $1.4 M_{\odot}$ ejecta.

Table 1. Simulation Parameters

Parameter	Case A	Case B	Case C
n_0	0.2	0.01	0.002
$T_0(\text{K})$	5×10^6	10^7	5×10^7
$r_{init}(\text{pc})$	1.0	5.0	2.0
$c_s(\text{km/sec})$	339	479	1071
$t_c(\text{Myr})$	0.035	0.053	0.024
$M_{\text{swept}}(M_\odot)$	874	437	87
$t_{M=2}(\text{Myr})$	0.016	0.024	0.011